Establishing the fracture properties of delaminating multilayered decorative coatings on wood and their changes after consolidation with polymer formulations

Nanke C. Schellmann · Ambrose C. Taylor

Abstract In the field of cultural objects conservation efficient stabilisation of fragile and failing, multilayered decorative coatings is a complex and challenging task. This paper introduces a new application of the standardised double-cantilever beam (DCB) test method to improve the understanding of the mechanical properties of failing material and to determine the effect of polymeric agents (consolidants) added for their stabilisation. The adapted DCB method was used to measure the fracture energy, G_{Ic}, and the fracture behaviour of brittle, protein-bound (gesso-type) foundation layers on wooden substrates that typically suffer from delamination and flaking. Wooden DCB specimens containing a brittle layer of protein glue mixed with finely ground clay powder were prepared, fractured, then consolidated with a range of commonly used polymer formulations and finally re-fractured to provide measurements for direct comparison. Consolidants tested included gelatine-based glues (bovine hide glue, isinglass; both pre-stained with Fast Green dye), acrylics (Lascaux Medium for Consolidation, Paraloid B-72/B-48N), poly(vinyl acetates) (Mowilith 50, Mowilith DMC2) and poly(vinyl alcohol) (Mowiol 3-83). Before second-phase fracture cross-sections were taken from the DCB specimens for determining penetration depth and gap-filling ability. For better visibility, the specimens containing acrylics were stained with Solvent blue G dye; iodine-potassium iodide was used for staining the other synthetic consolidants. The resulting data showed that the test method could determine measurable differences between initial G_{Ic} (47 ± 22 J/m^2) and post-consolidation G_{Ic} values. Also, penetration behaviour could be well characterised and valuable, and detailed information on the type and location of crack path propagation was gained.

N. C. Schellmann
Institute for Conservation-Restoration, Academy of Fine Arts Vienna, Schillerplatz 3, 1010 Vienna, Austria
e-mail: n.schellmann@akbild.ac.at

N. C. Schellmann (✉)
SchellmannConservation, Hohenzollernstrasse 29, 80801 Munich, Germany
e-mail: studio@schellmannconservation.com

A. C. Taylor
Department of Mechanical Engineering, Imperial College London, South Kensington Campus, London SW7 2AZ, UK
e-mail: a.c.taylor@imperial.ac.uk

Introduction

Background

Decorative coatings on wooden substrates are found on a great variety of cultural (art) objects throughout the world, ranging from furniture and sculptures to panel paintings and architectural elements. Characteristically, many of these coatings are composed of multiple layers which often consist of different materials that have greatly varying properties. Upon ageing and exposure to unsuitable environmental conditions, these coatings can degrade and lose their physical integrity. Over time, this can lead to increasing damage and may eventually render the objects entirely unsuitable for their intended use. The ageing processes and subsequent failure of such structures are typically of a complex nature but are often manifested in the development of delamination and lifting of coating layers.

To preserve these coatings and objects, efficient stabilisation of their fragile and failing elements is required. This, however, is a complex and challenging task. In the conservation of cultural heritage objects, high demands are made on the polymeric stabilising agent (the consolidant) used to achieve effective strengthening of the decorative coatings:

In many cases where porous materials require stabilisation, the polymeric consolidant added to the structure is required to serve two functions. Firstly, the polymer acts as an adhesive where layers are delaminating due to adhesion failure or fracture between individual layers of the structure. Secondly, it acts as a consolidant (i.e. strengthening agent) within one or several layers that are disintegrating due to cohesion failure within the layer material itself. As in practice the actions of re-adhesion and internal material strengthening can rarely be strictly separated from each other, the same polymer may often be used for both purposes. However, to ensure good gap-filling and/or penetration, respectively, the concentrations and viscosities are often adapted.

Furthermore, a suitable stabilisation treatment should not only appropriately strengthen the object, but also slow down significantly its further course of deterioration. This means that no additional degradation should be induced by the material added during treatment or in the future, as specified by the relevant professional standards and guidelines [3, 4]. Conservators are hence required to predict the performance of a potentially suitable consolidant, which in turn necessitates a thorough understanding not only of the properties of both the consolidant and the fragile material in isolation, but also of the stabilised material as a composite.

Unfortunately, information on these characteristics is usually scarce or entirely unavailable, as the component materials of art objects are rarely standardised: they are generally inhomogeneous, as they are frequently sourced from natural sources that can be variable and typically produced and processed by hand in little standardised or poorly documented ways. Consequently, reliable technical data on the object's materials are often unknown [5; chapter 4]. Furthermore, by the time such objects require conservation, the materials are usually aged, and their properties will have changed in various ways and to varying degrees [6, 7; chapter 8].

In addition to the lack of information on the material to be consolidated, the properties of the polymeric consolidants and adhesives available are mostly, if at all, known only for the bulk material but not when dispersed in a porous coating and potentially containing numerous voids [8].

This paper therefore investigates a new approach for the evaluation of the performance of the polymer formulations employed to consolidate fragile decorative coating structures, by looking at the fracture properties of a model coating before and after consolidation. Here, the polymer is required to act both as an adhesive and as a consolidant. For illustration purposes, this research was performed on model East Asian (*urushi*) lacquer coating structures containing protein-bound foundation layers. These present a typical example of multilayered decorative coatings that are highly prone to delamination and flaking [9].

Conventional strength of materials testing versus the fracture mechanics approach

In the field of art and decorative objects conservation, the strength properties of materials are most commonly characterised in bulk using quasi-static tensile, compressive or flexural tests [10–14], whilst adhesive joints are usually analysed using peel, tensile or shear tests [15–23]. However, whilst these tests are simple to perform, they are not necessarily ideal for evaluating polymers for conservation purposes, as they do not characterise well the performance of these polymers as consolidants. Firstly, the strength values gained from conventional tests are dependent on the specimen geometry and the test conditions used, thus not allowing for universal comparison. For example, the tensile strength of brittle materials varies depending on the depth of scratches on the surface. Secondly, these tests often do not satisfactorily model the failure observed on real-life objects. For example, it is easily acknowledged that an adhesive joint between two carefully prepared, clean, flat surfaces (as required for most conventional mechanical strength test specimens) will perform significantly differently from that between two fractured, rough surfaces that need consolidation and re-adhering. Furthermore, the fracture properties and the forces leading to failure differ depending on the direction of specimen loading. It is therefore important to consider which loading conditions in mechanical strength tests will provide stresses that most suitably simulate those which lead to failure in an object during service.

In multilayered coatings, the inter-laminar plane has the lowest resistance to fracture, so failure generally develops parallel to the laminar structure. Consequently, the most likely failure scenario for a coating would be delamination in mode I, which of the three loading conditions requires the least amount of energy to induce fracture [24, p. 311]. The pervasiveness of this fracture mode on real-life objects was observed during a survey of damaged East Asian lacquer-coated furniture in the collection of the Victoria and Albert Museum in London, which identified severely delaminating and flaking coating layers on a range of objects [5, 9]. With regards to the re-adhesion and consolidation of such layered structures, which are desired to fail in the future along the line of the already consolidated fracture, if at all, and not by failure in new areas, it is thus a

useful approach to investigate the fracture resistance of a coating material under mode I conditions. Only fracture mechanics can characterise this failure adequately, as the testing does not initiate immediate catastrophic fracture but rather slow failure as seen in real objects.

Materials and methods

Mode I testing

Although the basics of the test method outlined here are well known in adhesives testing, e.g. [25–31], the novelty of its use for conservation and the variations used in the present work demand that a fuller explanation of the technique is provided.

The fracture energy in mode I (G_{Ic}) is an independent material property. To measure G_{Ic}, a rather simple specimen, the double-cantilever beam (DCB) specimen, is tested in tensile loading following a standardised method [32]. Details of the specimen containing the material or joint to be tested between the substrates are given in Fig. 1. The DCB is pre-fractured to a few millimetres beyond the starter foil to create a sharp crack tip. This pre-cracking is essential as G_{Ic} values measured from the insert may be unrealistically high as even a thin insert may be insufficiently sharp for brittle materials [33]. After full unloading, the specimen is re-loaded, and crack propagation is monitored whilst recording the applied load and displacement. These data allow the energy required to initiate and propagate a crack to be calculated. Additionally, information is gained on the stability of the crack growth, indicating whether a crack grows catastrophically or in a slow and steady manner. DCB specimens with sufficiently long substrates allow the uniformity of the material or the adhesive bond to be evaluated, as crack initiation and arrest can be observed repeatedly over a considerable distance.

A significant advantage of this test method is that the specimens can be repaired after initial fracture and be re-tested. During the first experiment, information is gained on the fracture behaviour of the coating material. If the specimens are then consolidated with polymer formulations and fractured a second time, data on the composite's (i.e. the artist coating material/polymeric consolidant) fracture and mechanical properties after consolidation are obtained. This allows a direct evaluation of the changes in mechanical performance of the coating induced by the tested consolidant.

Test specimens

The test specimens were designed and prepared in a procedure that was based on traditional practice but was adapted to provide more controlled uniformity and reproducibility. Two types of test specimens were prepared: firstly, a very simplified type (Type A) containing an 'adhesive' layer made from a mixture of mammalian hide glue and Japanese clay powder (gesso-type foundation) between two wood substrates. A second type of samples (Type B) incorporated an additional lacquer layer between the foundation and one of the wooden substrates.

For the DCB specimen substrates, boards (lamina) of 5 mm thickness were cut with a circular saw from a flat-sawn, finely grained, knot-free and well-seasoned log of Québec yellow pine (*Pinus strobus*) at 3° to the wood grain. The latter ensured a consistent modulus of elasticity in each beam and helped direct the crack away from the substrates during testing, e.g. [34]. Two boards of consecutive lamina were paired together, orientating the grain angle in a 'V' shape towards their boundary (Fig. 2).
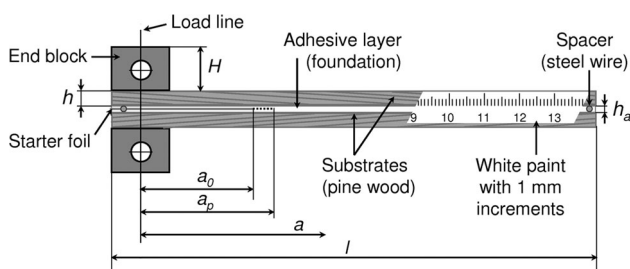

Fig. 1 DCB specimen with end-blocks according to BS7991 [32]. *l* total specimen length (150 mm), *h* thickness of the wood substrate (4 mm), h_a thickness of the adhesive (foundation) layer, *H* thickness of the end-block (13 mm), a_0 starter foil length from the load line (30 mm), a_p pre-crack length, measured from the load line to the tip of the pre-crack, *a* crack length, measured between the load line and the observed crack tip (>30 mm)
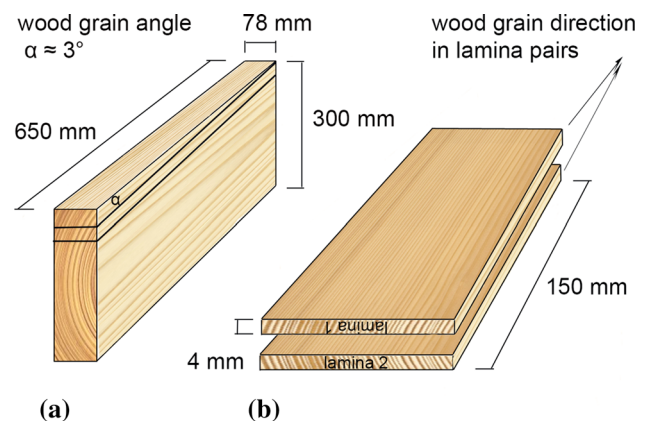

Fig. 2 **a** Cutting of laminae from pine wood log at a 3° grain angle, **b** pairing of consecutive laminae showing V-shaped alignment of wood grain on the length-side surface

The foundation was a mixture of bovine hide glue (Kremer Pigments) and the Japanese clay powder *tonoko* (Dictum). A 10 weight percent (wt%) solution of hide glue was prepared by stirring at 60 (±1) °C water temperature for 30 min. The finely ground and sieved *tonoko* was slowly added to the warm glue solution to a weight ratio of 1:1. The mixture was filtered through fine gauze (15 den polyamide tights) and swiftly applied to the wood boards in an approximately 0.5-mm-thick layer using a soft-haired brush.

For the Type A specimens, the warm foundation mixture was applied to a pair of wood boards of dimensions 150 mm by 78 mm. A 12.5-µm-thick polytetrafluoroethylene (PTFE) starter foil was immediately placed at the end of one coated board (at the open side of the 'V' shaped grain angle), and two 0.25 mm diameter stainless steel wires were positioned at each end as spacers (Fig. 1). The second board was then placed on top (foundation side down), and the bonded specimen board was moved into a steel press pre-warmed to 30 °C, where it was left under a pressure of approximately 0.4 MPa at 21.0 (±1.5) °C for 16 h.

Type B specimens were prepared by applying the warm foundation mixture in two consecutive layers to only one board of each substrate pair. After drying, the foundation was ground with 150 grit emery paper until the surface was even and then coated with five layers of East Asian lacquer (Chinese *ki urushi*, Watanabe-shoten/Tokyo), applied in the traditional manner in very thin layers using a v-shaped Japanese human hair brush. In-between each application, the specimen board with the lacquer coating was placed inside a humidity chamber at 74.0 (±1.5) %RH at 21.0 (±1.5) °C for the lacquer to polymerise. A PTFE starter foil was incorporated at one end of the specimen board after application of the second lacquer coating layer. The second wood substrate was subsequently adhered to the top lacquer surface using a room-temperature curing epoxy adhesive (Araldite 2015, Huntsman) and the specimen placed in a press at a pressure of approximately 0.6 MPa at room temperature for 24 h.

The DCB specimens were cut from these sandwiched boards using a bandsaw and ground using 150 grit emery paper to final dimensions of 20 mm in width and 150 mm in length. All specimens were equilibrated at 53.0 (±1.5) %RH at 21.0 (±1.5) °C for three months before testing. The specimens were weighed at regular intervals, and full equilibration was determined after 2 months when their mass ceased to change significantly (i.e. changes of <0.0015 % per 24 h).

Before testing, aluminium end-blocks were attached using a cyanoacrylate adhesive (Loctite super glue, Henkel). A thin coat of proprietary solvent-based white paint (correction fluid) was applied across each specimen's bond-line with a paper scale marked in 1 mm increments for easier monitoring of crack propagation during testing (Fig. 1).

Choice of consolidants for pre-fractured DCB specimens

After initial fracture (cf. 'Fracture testing' section below), the DCB specimens were re-adhered using various polymer formulations (consolidants) to provide specimens for second-phase fracture. The polymers were chosen based on a review of the chemical and physical factors that determine the properties of various consolidants typically used for failing coating structures in the field of art conservation [5; chapter 4]. The choice comprised polymers from different classes and some mixtures (i.e. proteins, polysaccharides, acrylics, poly(vinyl acetate) (PVAc) and poly(vinyl alcohol) (PVAl)) and included both aqueous and hydrocarbon solvent-based (polar and non-polar) formulations. The exact choice of the polymers was based on successful experience of previous research reported by the author in the before-mentioned review. Ten different polymer formulations were chosen for testing (Table 1). The individual polymer concentrations were tested and selected in pretests so that the formulations had roughly comparable working properties such as a sufficiently low viscosity to allow even spreading and were able to bond the specimens without their failing during simple handling.

Staining and application of consolidants

Staining was used to indicate the depth of penetration and distribution of the consolidant within the foundation, by examination in cross-section using microscopy. Where the consolidant could be stained prior to application, it also indicated the proportion of fracture which occurred in the treated foundation rather than the unconsolidated coating material.

The protein-based formulations were stained with Fast Green [35, pp. 214–216] and the acetone-dissolved acrylic with Solvent Blue G stains, respectively, prior to application. Cross-section samples were cut from the far ends of the DCB specimens before second-phase fracture testing (Fig. 1). The cross-sections were polished and examined with incident visible light using an optical microscope (Zeiss AxioScope A1, reflected light geometry). The remaining consolidants were stained on the cut cross-sections, using Solvent Blue G stain in ethanol for the acrylics, and iodine-potassium iodide (Lugol's) solution for the starch, PVAc and PVAl consolidants [36], as shown in Table 1.

The consolidants were applied using a flat, 20 mm wide bristle brush to both fracture surfaces of four DCB specimens each. Application was with three brush strokes of a freshly loaded brush for each fracture surface, to give an

Table 1 Consolidants used for DCB specimens

Type	Polymer	Solvent/diluent	Concen-tration (wt%)	Refs.	Set No.	Stain
Protein	Isinglass (from sturgeon-bladder)	Water	10	[50]	A1 B1	Fast Green (0.1 wt%), added to consolidant
	Fish glue (proprietary, cold-liquid)	Water	22.5	[48, 51, 52]	A2	Fast Green (0.1 wt%), added to consolidant
	Bovine hide glue	Water	10	[50, 53]	A3 B3	Fast Green (0.1 wt%), added to consolidant
	Isinglass/wheat starch paste	Water	13.3	[42, 43]	A4 B4	Fast Green (0.1 wt%), added to consolidant/ cross-section stained with Lugol's solution
Acrylics	Paraloid B72 (EMA/MA/nBMA)	Toluene	25	[54–56]	A7	Solvent Blue G, cross-section stained with 0.2 wt% in ethanol (exposure time 10 min)
	Paraloid B72	Acetone	25	[57]	B7	Solvent Blue G (0.1 wt%), added to consolidant
	Paraloid B48N (MMA/BMA)	Toluene/xylene (1:1)	25		A8	Solvent Blue G, cross-section stained with 0.2 wt% in ethanol (exposure time 10 min)
	Lascaux MfC	Proprietary aqueous dispersion, undiluted	25	[45]	A9 B9	Solvent Blue G, cross-section stained with 0.2 wt% in ethanol (exposure time 3–5 min)
PVAl	Mowiol 3-83	Water	25	[54]	A10 B10	Lugol's solution (exposure time 3 s)
PVAc	Mowilith 50	Toluene	20	[58]	A11	Lugol's solution (exposure time 3 s)
	Mowilith DMC2 (35 % dibutyl maleate)	Proprietary aqueous dispersion + water	10		A12	Lugol's solution (exposure time 3 s)

The letters in the set numbers denominate the type A or B specimens that were tested

equal and even distribution of the consolidant. The two beams were placed together, and the DCB specimen was moved into a press at 23 kPa for 2 days at room temperature, before being transferred into the humidity-controlled chamber for equilibration as described earlier. Equilibration times until testing were 2.5 and 3.5 months for type A and B specimens, respectively (the varying times solely being a consequence of testing equipment availability).

Mode I fracture testing

The adhesive fracture energy, G_{Ic}, was measured according to the British Standard [32] using an Instron 5584 universal testing machine fitted with a 5-kN loadcell and a humidity-controlled chamber. The tests were performed at a monotonic cross-head displacement rate of 0.3 mm/min and at 53.0 ($\pm$0.5) %RH and 21 ($\pm$1) °C. The applied load at fracture, P, displacement, δ, and crack length, a, was recorded (Fig. 1), and G_{Ic} was calculated using the corrected beam theory method [32]:

$$G_{Ic} = \frac{3P\delta}{2B(a + |\Delta|)} \cdot \frac{F}{N},$$ (1)

where B is the specimen width. The correction factors Δ, F and N correct for the beam not being perfectly built-in at

the crack tip, for large displacements and for the stiffening effect of the end-blocks, respectively. Their values are specific for each specimen and are calculated as defined in the Standard [32]. The data analysis was undertaken using a spreadsheet provided by Blackman and Kinloch [37, 38].

Experimental results

Introduction

To establish the effect of the consolidants on the fracture behaviour of the specimens, the fracture surfaces and fracture energy values, measured after consolidation, were compared to those from the initial testing. Complementary data on the distribution of the consolidants in the foundation were gained from cross-section analysis:

Results of initial fracture of the foundation

During initial testing of the foundation, the DCB specimens mostly exhibited stable crack propagation. In a few instances, some unstable fracture was observed during testing where the crack jumped, propagating fast over a short distance before arresting. These instabilities, caused

by inhomogeneities in the material, were mainly associated with variations in the fracture paths. The latter had either propagated mostly cohesively through the foundation layer or adhesively (interfacially) between the foundation and the wood. Most commonly, the fracture surfaces on a single specimen showed both cohesive and interfacial failure (Fig. 3). Where cohesive failure occurred, the fracture path was observed to often propagate on varying levels through the layer. The fracture surfaces display a striking resemblance to those found on real-life objects involving similar foundation layers, which often show complex failure patterns featuring both cohesive failure on multiple levels and interfacial failure (Fig. 4).

The variable crack growth stability in the DCB specimens observed during testing clearly showed in the analysed data. For stable crack growth, the load versus displacement graph shows a relatively smooth decrease in load during crack propagation, whilst the crack length increased almost linearly. A typical example is shown in Fig. 5 (square data points/stable data). The graph plotting the calculated fracture energy values versus the crack length shows uniform propagation close to the mean value (Fig. 6). In contrast, the unstable crack growth observed in a small number of specimens gave a less-smooth decrease and more variation in the graph of G_{Ic} versus a, together with a step-like rise of the a versus δ graph. An example of very unstable crack propagation is given by the red curves (diamond data points/unstable data) in Figs. 5 and 6. As these instabilities had little effect on the overall measured G_{Ic} values, this behaviour was deemed acceptable for such an inhomogeneous material and the measured values were simply averaged.

The average fracture energy of all tested protein-bound foundation layers was 46 ($\pm$12) J/m^2 for type A and 47

Fig. 4 Detail of typical coating loss on a nineteenth century Japanese export-type lacquer cabinet in the V&A collection (V&A 303-1876, courtesy of the Victoria and Albert Museum, London)
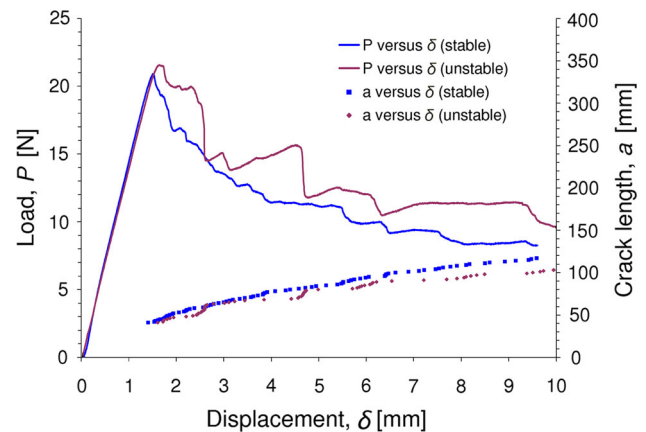

Fig. 5 Load-displacement and crack length-displacement curves for two DCB specimens during initial fracture showing stable and unstable crack growth [1]
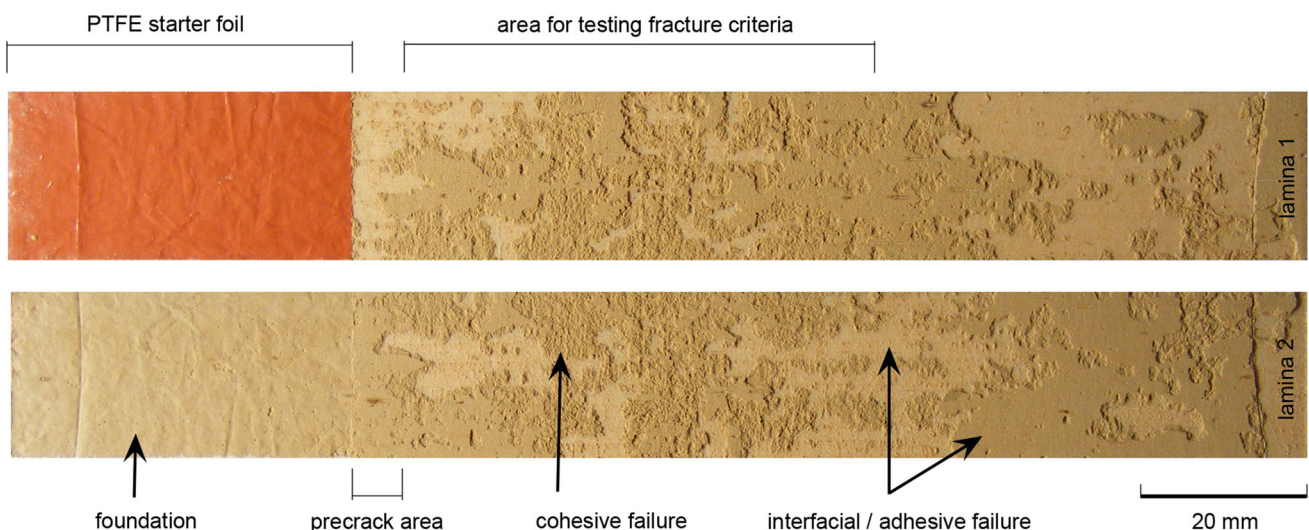

Fig. 3 DCB specimen fracture surfaces of the foundation material after initial testing showing typical failure
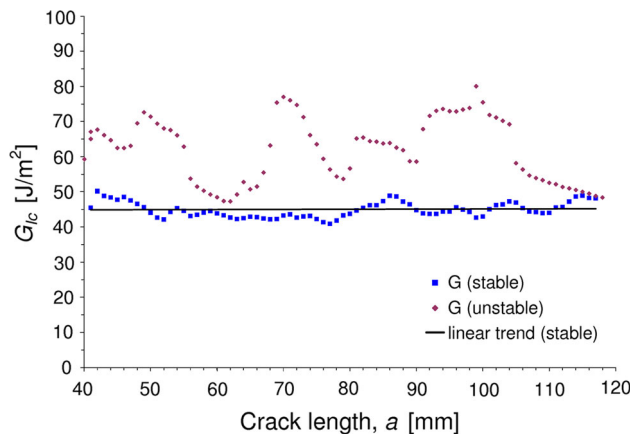
Fig. 6 Fracture energy versus crack length curves for the same specimens as in Fig. 5 during initial fracture, showing near constant G_{Ic} over specimen length for stable fracture and variable G_{Ic} during unstable crack propagation [1]

($\pm$22) J/m^2 for type B specimens. Apart from the higher standard deviation for type B specimens, which is not unexpected for such inhomogeneous material [34, 39], there is no significant difference between the measured G_{Ic} values, and hence 47 ($\pm$22) J/m^2 will be used from here on. This is a typical value for such a material. Numerical values for the fracture properties of composites made from mammalian glue with mineral particle fillers are not available for comparison; however, comparative data may be drawn from other highly filled polymers. Friedrich and Karsch [40], for instance, demonstrated that above a filler concentration of 15 vol% the fracture energy of silicon dioxide-filled polypropylene decreased rapidly, reaching similarly low values at high filler concentrations as the mammalian glue-bound foundation in the present study.

The aim of the initial testing, to produce DCB specimens with fracture surfaces that provide appropriate specimens for the further testing of consolidant performance, was thus achieved. After this round of testing, all specimens were consolidated as described above and second-phase fracture testing was undertaken.

Results of second-phase fracture after consolidation

The retesting of the consolidated specimens gave more variable data than the initial testing. This variability resulted from more unstable crack growth due to increased specimen inhomogeneity, which was expected from a damaged, porous material stabilised by simple brush-application of a consolidant which may not have penetrated fully through the foundation. Nevertheless, the overall reproducibility of the data was reasonable. Clear trends could be deduced, and direct comparison between the calculated G_{Ic} values, the fracture surfaces and the crack growth rate stability from pre- and post-consolidation

testing gave valuable results on the effects of the polymer formulations used as consolidants. The following sections will summarise the results and present examples of typical data for illustration purposes.

Fracture surfaces

Examination and evaluation of the fracture surfaces were undertaken by eye and using a jig with gridlines to calculate area percentages of failure types. The percentage of new failure created after second-phase fracture gave information on whether the fracture occurred within the bondline between the old fracture surfaces or in entirely new areas of the foundation. These results indicated whether the consolidants were efficient bonding agents for joints of the old fracture surfaces and whether they were likely to facilitate the undesirable failure of new areas of the material. This is important because conservation is usually aimed at creating bondlines that effectively stabilise or strengthen the structure but that tend to be weaker than the surrounding original material, so as to avoid or limit any new damage in original, yet unfractured parts of the object upon further exposure to unfavourable environmental conditions and situations [3, 4, 15].

Figure 7 shows examples of typical DCB specimen types A and B after initial (Fig. 7a, c) and second-phase fracture (Fig. 7b, d). The differences in the fracture paths are readily discerned: the fracture surfaces show a high proportion of cohesive failure (CF, fracture within the layer) partly within the consolidated (green-stained in Fig. 7b, darker areas in Fig. 7d) and unconsolidated areas (unstained areas in Fig. 7b, lighter areas in Fig. 7d) of the foundation, as well as some new interfacial, i.e. adhesive failure (AF) between the foundation and the wood substrate, and some failure between the old, re-adhered fracture surfaces. A summary of the results for all specimen sets is presented in Fig. 8.

Fracture energy

The average G_{Ic} values for all specimen sets before and after consolidation are summarised in Fig. 9. The very first bar in each chart represents the overall mean fracture energy of all the type A and B DCB specimens during initial fracture (47 J/m^2). The consecutive pairs of bars refer to the initial and post-consolidation fracture of the four specimens used in each set. The right-hand bars of each set indicate the performance of the consolidants, i.e. the averaged fracture energy for the set, assuming that all the test specimens were more or less equal in their properties before consolidation treatment. Comparison of the initial and post-consolidation bars enables a direct evaluation of the overall consolidation performance for each set.
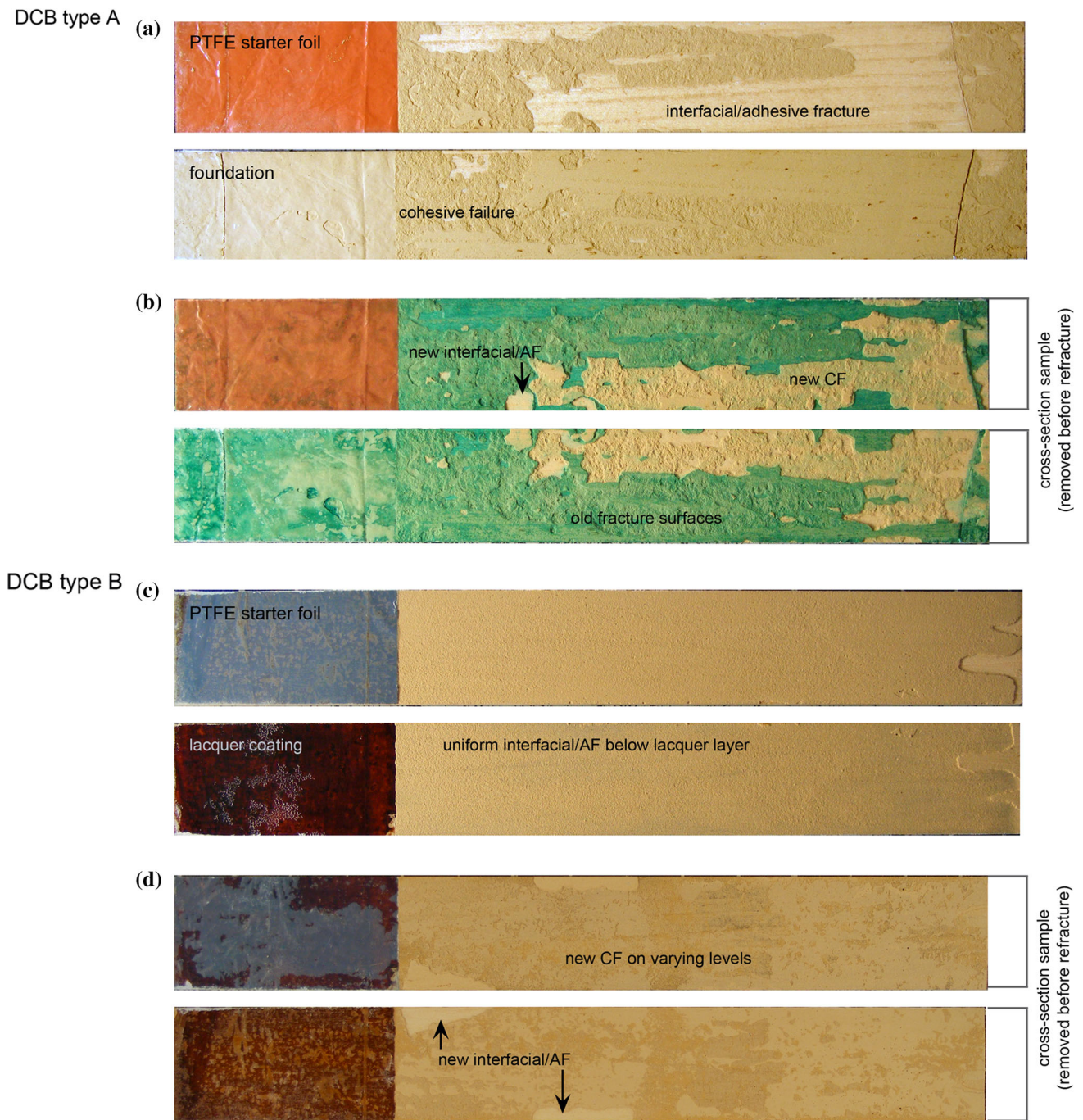
Fig. 7 DCB specimens after initial and second-phase fracture; **a** specimen type A after initial fracture; **b** after second-phase fracture post-consolidation with isinglass/starch stained with Fast Green; **c** DCB type B after initial fracture and **d** after consolidation with Lascaux Medium for Consolidation. The fracture surfaces of **b** show some new cohesive failure (CF) mainly in unconsolidated (unstained) areas of the foundation, as well as little new interfacial, i.e. adhesive failure (AF) between foundation and wood substrate, and some failure between the old, re-adhered fracture surfaces. The fracture surfaces of **d** show predominantly new cohesive failure on varying levels within the foundation layer and little new interfacial/adhesive failure

To account for the large variability in the inhomogeneous samples across each individual set and to correct the absolute mean G_{Ic} values from the systematic error contained within, the relative changes in fracture energy (for each individual specimen before and after consolidation), ΔG_{Ic}, were also compared, as shown in Fig. 10.

From the bar graphs in Figs. 8, 9, and 10, it can be seen that the cold-liquid fish glue (set A-2), the three Paraloid
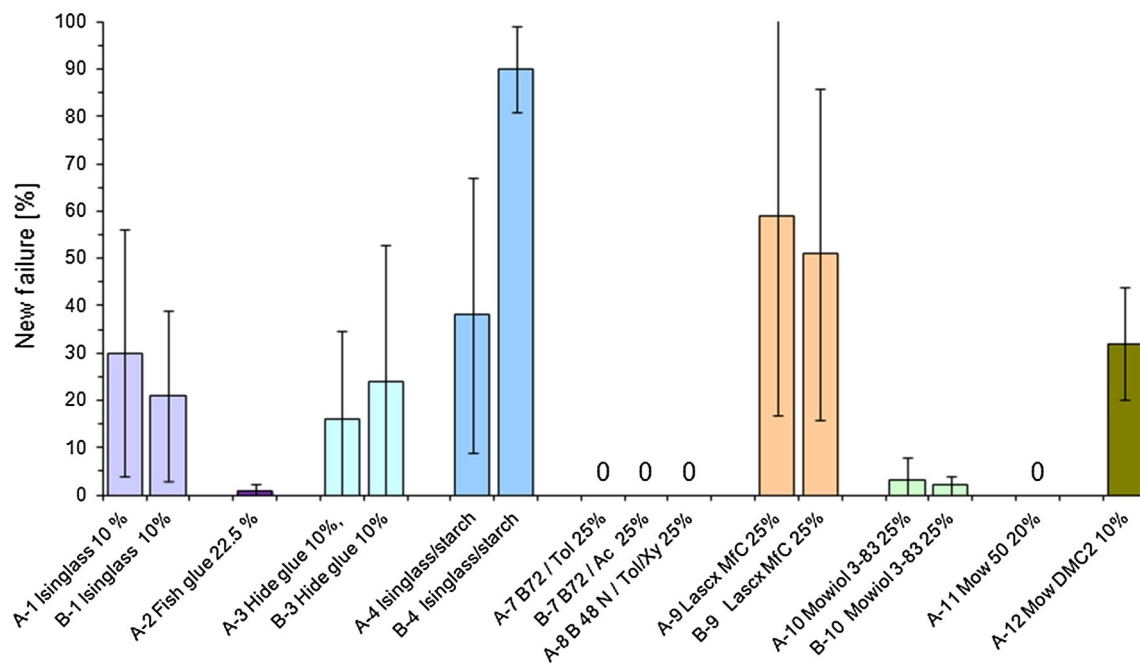
Fig. 8 Percentage of failure in new areas of the DCB specimens recorded after second-phase fracture. The remaining failure developed within the bondline, following the fracture path from initial testing either within the bulk consolidant or within the joint starved of consolidant/adhesive. *Error bars* indicate ± one standard deviation

solutions (sets A-7, A-8 & B-7) and the Mowilith 50 (set A-11) all failed to strengthen the specimens. Figure 8 shows that fracture almost unanimously occurred in the bondline, due to the consolidants' lack of adhesive and/or gap-filling abilities. In the specimens consolidated with the fish glue (set A-2) and the Mowiol 3-83 (sets A-10 & B-10) less than 2 % of the fracture surfaces were located in previously unfractured areas of the specimens, whilst the specimens consolidated with the Paraloid solutions showed virtually no failure outside the bondline of the re-adhered surfaces. No significant difference at all was observed in the performance of Paraloid B72 dissolved in acetone (set B-7) and those Paraloid formulations dissolved in the benzenes (toluene and toluene/xylene). Even though differences in the mechanical performance of the consolidants could have been expected due to the differential polarity and solubility parameters of the solvents, e.g. [7; chapter 12], these did not show in these tests (see also Figs. 9, 10). This similar behaviour may hence be fully attributed to the insufficient gap-filling ability of the Paraloid solutions, which had left the joints starved of adhesive despite their relatively high solution concentration of 25 % solid content. This suggests that single applications of solvent-based consolidant-formulations may be insufficient to re-adhere such porous fracture surfaces.

The PVAl Mowiol 3-83 displayed some degree of strengthening, despite not being able to restore G_{Ic} to the original level measured during initial fracture (Fig. 9). Results for types A and B specimens were practically the

same, both showing failure almost entirely within the bondline (Fig. 8) and at G_{Ic} levels of around half their original value.

The remaining protein-based consolidants (except for the cold-liquid fish glue) showed partly similar and partly differing performance. For the type A specimens (sets A-1, A-3 & A-4), all the consolidants showed overall fracture energy values more or less equal to those measured during initial fracture (Fig. 9). As would be expected, only the scatter of the data tended to be larger after consolidation. The ΔG_{Ic} values for type A specimens were generally small (Fig. 10), indicating no significant changes.

At first glance, the behaviour of the protein-based consolidants appears to differ between the type A and type B specimens. The isinglass and hide glue seem to show opposite results for ΔG_{Ic}. However, when the experimental variation is considered, the results are fully within the range of the standard deviation of the type B specimens, which is relatively large (Fig. 10). Thus, the respective positive and negative changes are not contradictory. Both consolidants also showed similar amounts of fracture in new areas of the specimens (Fig. 8). However, the isinglass/starch achieved exceptionally high levels of new failure in the type B specimens, also reflected in the significantly higher fracture energy values for the type B specimens compared with type A. The generally higher mean fracture energies for type B specimens than for type A raise the question of whether the longer equilibration times for these specimens played a significant role in

Fig. 9 Mean fracture energy, G_{Ic}, values for each DCB specimen set of **a** type A and **b** type B, before and after consolidation. *Error bars* indicate ± one standard deviation (Fig. 9a, [2])
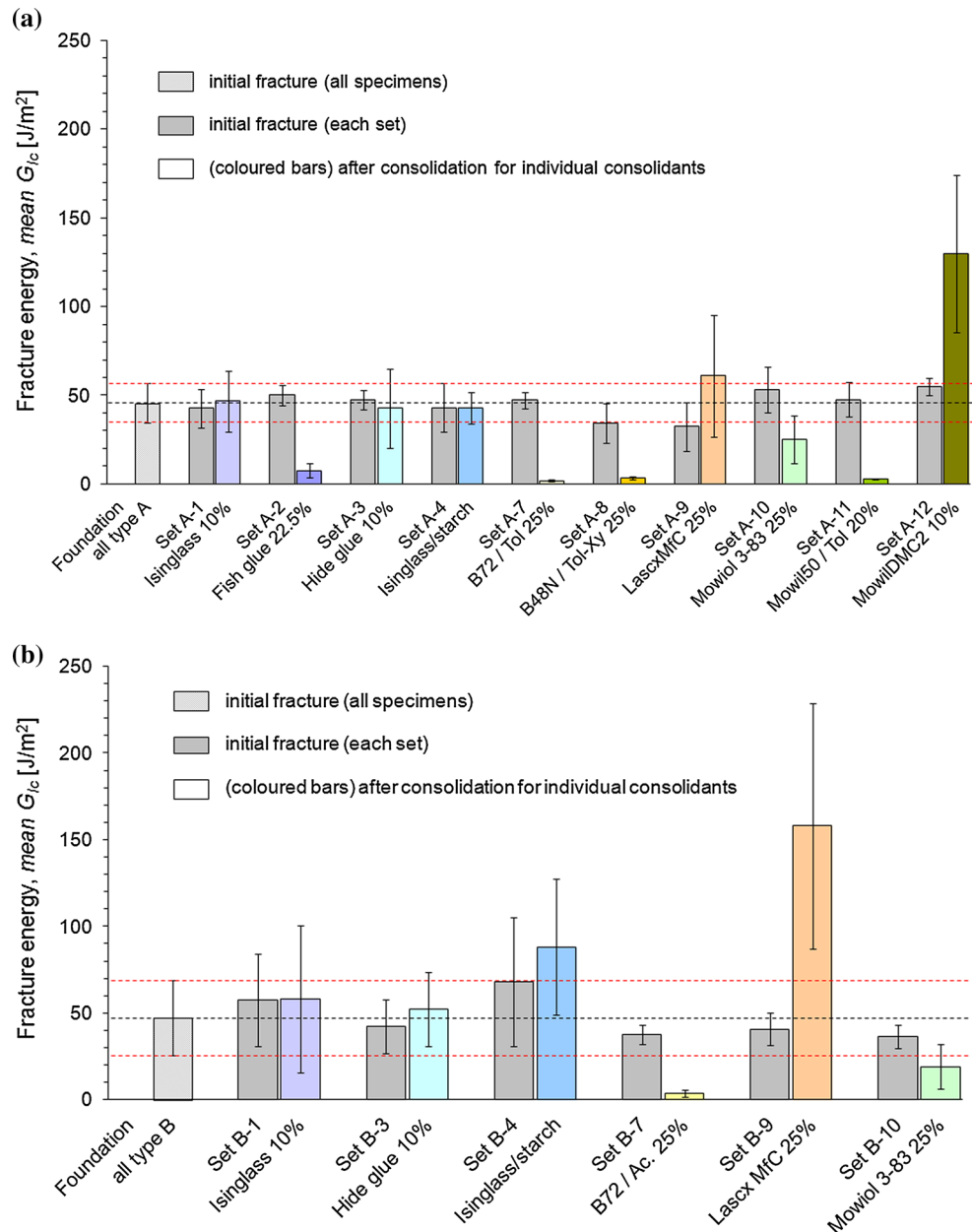
achieving higher values during fracture testing. It is likely that the additional month of curing for the consolidants continued to toughen the specimens.

The largest average increases in G_{Ic} were measured for the polymer dispersions Lascaux Medium for Consolidation (acrylic, set A-9 & B-9) and Mowilith DMC2 (PVAc-based, set A-12). Levels well above 100 % of their original value were reached for the type A specimens, whilst for type B, the Lascaux MfC showed mean increases up to 180 % (Fig. 10). Lascaux MfC displayed an overall greater percentage of fracture in new areas of the foundation compared with Mowilith DMC2 (Fig. 8). Together with a greatly increased fracture energy relative to that of the unconsolidated foundation (Figs. 9, 10), this implied that

the Lascaux MfC had not only re-adhered the fracture surfaces well, but had also effectively strengthened the foundation layer far beyond its original properties.

Again, the significantly increased G_{Ic} values for Lascaux MfC type B specimens were attributed to the longer equilibration time of the samples. The mechanical properties of polymer dispersions were shown to change significantly during the first (at least 3.5) months after application [5].

Penetration behaviour

A qualitative indication of each consolidant's performance was gained by measuring the bondline thickness and assessing the penetration ability of the consolidants by

Fig. 10 Effect of consolidants expressed as mean relative changes in fracture energy, ΔG_{Ic}, measured during second-phase DCB testing. *Error bars* indicate ± one standard deviation
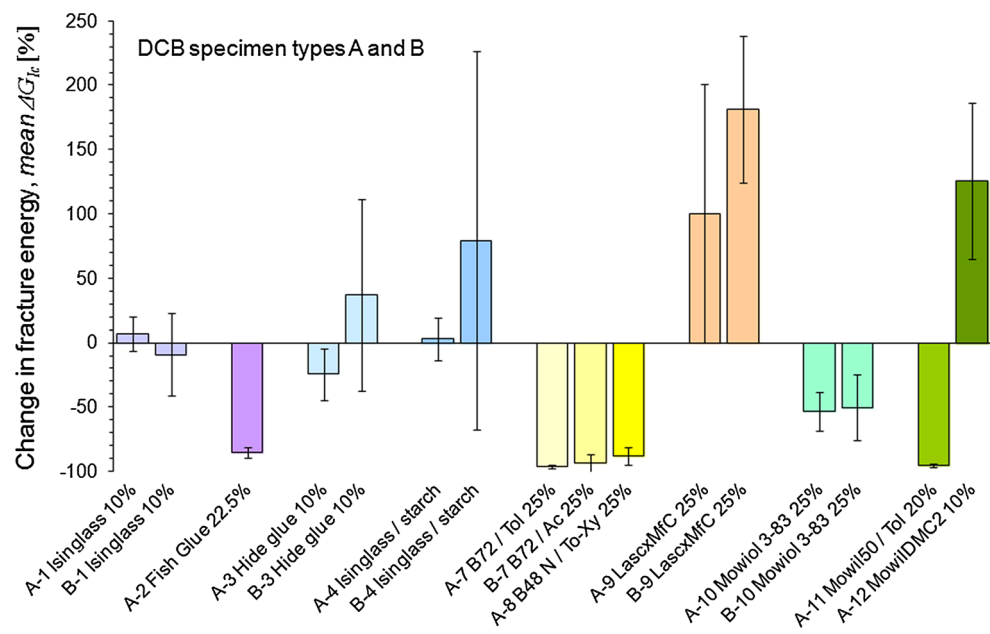
cross-section microscopy of the DCB specimens. The penetration depth was ascertained from the micrographs by evaluating the distribution of the individual stains used. Intense- or dark-coloured areas were interpreted as containing a high consolidant concentration and areas appearing lighter coloured as containing lower concentrations. In many cases, the penetration was graduated from high at the bondline to low further away from the bondline. Here, the penetration depth was measured to the furthest point where the stain was still discernible with the human eye using the microscope. In the specimens containing the protein consolidants pre-stained with Fast Green, it was assumed that the stain distribution was not biased by chromatographic effects.

The average foundation layer thickness before consolidation was 0.32 mm for both type A and type B (excluding the lacquer and epoxy polymer layers). Examples of typical cross-section micrographs are presented in Fig. 11. A type B specimen consolidated with isinglass/starch, stained with Fast Green is shown in Fig. 11a, and displays almost complete penetration of the stained consolidant through the entire foundation layer down to the wood interface. Figure 11b presents a type A specimen consolidated with Lascaux Medium for Consolidation, stained with Solvent Blue G, that demonstrates more limited consolidant penetration (in the grey-blue zone) marked with a double-headed white arrow. The single (white) arrows mark the bondline between the re-adhered fracture surfaces.

Broad trends of consolidant bondline thicknesses and penetration depths were established for each DCB specimen set, and the results are summarised in Table 2. The data give the overall mean results for both specimen types

A and B. This summary shows that the non-aqueous consolidants mostly displayed insufficient adhesive bonding between the fracture surfaces and thus failed at the given concentrations as effective consolidants for fractured foundation layers. As mentioned earlier, this is explained by the fact that non-aqueous consolidants do not soften and swell the foundation layers, preventing imperfectly fitting fracture surfaces to adjust adequately to one another, and that single applications of solvent-based consolidants may be insufficient for preventing starvation of joints between highly porous surfaces. These findings are supported by Lencz's report [41] that multi-stage applications of acrylic solutions are required to successfully consolidate delaminating lacquer coatings. The cross-sections confirm that penetration of the hydrocarbon solvent-based consolidants is very high, backing the understanding that no effective bondline can be achieved with a single application. Two examples showing these phenomena are shown. Figure 11c presents a type A specimen consolidated with Paraloid B48N in toluene/xylene after staining with Solvent Blue G. A non-uniform distribution of the consolidant, with tide lines, extends through the entire foundation layer can be seen, with large voids and little consolidant bridging in the bond-line. In contrast, Fig. 11d shows the cross-section of a sample consolidated with Paraloid B72 in acetone, where penetration into the foundation layer is more limited, but the bondline between the fracture surfaces is still entirely starved of the polymeric consolidant.

The protein-based consolidants that were applied as warm solutions, i.e. hide glue (sets A-3 & B-3) and isinglass (sets A-1 & B-1), demonstrated ideal properties in that they allowed the fracture surfaces of the foundation
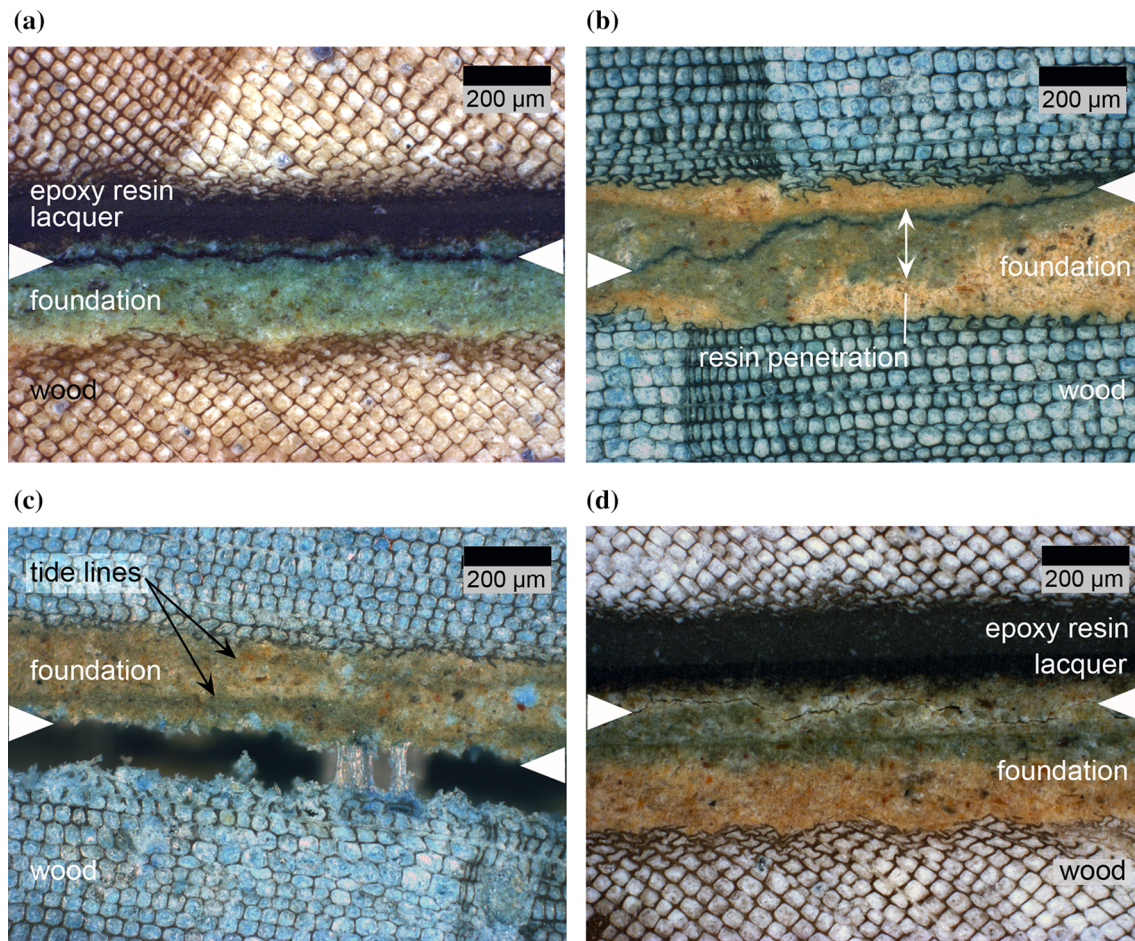
Fig. 11 Cross-sections of DCB specimens; **a** type B consolidated with isinglass/starch, stained with Fast Green; **b** type A consolidated with Lascaux Medium for Consolidation, stained with Solvent Blue G; **c** type A consolidated with Paraloid B48N in toluene/xylene and **d** consolidated with Paraloid B72 in acetone (type B), both stained with Solvent Blue G. *White arrows* on each side of the micrographs mark the bondline between re-adhered fracture surfaces, the *white double-ended arrow* in **b** highlights the limited penetration depth

layer to fit perfectly (due to softening of the layer). Also, they did not develop visible bondlines consisting of bulk polymer that could adversely influence the uniform distribution of mechanical properties in the consolidated layer. The isinglass/starch mixture showed both deep penetration and a significant bondline due to its two-phase composition of dissolved protein and dispersed agglutinated starch (Fig. 11a). These results confirm previous research by Breidenstein [42], who suggested after X-ray analysis of iodine-marked isinglass/starch-based consolidants applied to lacquer panels that isinglass/starch formed relatively thick adhesive layers underneath readhered lacquer flakes. A study by Springob [43] that had shown starch to be an effective thickening agent for isinglass was also confirmed.

A similar penetration ability of the water-based and acetone-dissolved consolidants was also observed, contrasting with the extensive penetration behaviour of the benzene-diluted (toluene and xylene) formulations through the full thickness of the layer. This was unsurprising considering the larger swelling capacity of polar solvents which hinders penetration in materials of the same polar nature, compared with that of non-polar solvents applied to the a polar system, e.g. [15, 44].

The most efficient gap-fillers were the Mowilith DMC2 and the Lascaux MfC, which also achieved the highest fracture energy values. However, despite this similarity and a much lower polymer content of the DMC2 dispersion (10 %), they showed rather opposing penetration behaviour, owing to greatly varying particle sizes. The Lascaux MfC contains relatively large particles of ∼0.03–0.3 µm in diameter [45], and at least some fraction of this dispersion will have difficulties in penetrating well into the foundation layer. In comparison, the DMC2 has even larger particles of ∼0.3–2.0 µm in diameter [46], hence will penetrate least and remain largely on the fracture surfaces, which was clearly visible in the crosssections.

Table 2 Summary of penetration and fracture behaviour of consolidants (mean values for type A and B specimens)

Type	Consolidant	Concentration (wt%)	Bondline thickness (μm)	Penetration depth into foundation (μm)	into wood (μm)	Gap-filling ability	Fracture energy, G_{Ic} (J/m²)	SD	Bondline failure (%)	SD
Protein	Isinglass (in water)	10	–	130–170	≤50	n.a.*	53	(±29)	75	(±20)
	Fish glue (in water)	22.5	Starved joint	100–200	≤50	Poor	8	(±4)	99	(±2)
	Hide glue (in water)	10	–	100–250	≤50	n.a.*	48	(±19)	80	(±21)
	Isinglass/starch (in water)	13.3	10–20	130–270	?	Excellent	66	(±33)	36	(±32)
Acrylics	Paraloid B72 (in toluene)	25	Starved joint	200–320	?	Poor	2	(±0)	100	(±0)
	Paraloid B72 (in acetone)	25	Starved joint	100–200	≤40	Poor	4	(±61)	100	(±0)
	Paraloid B48N (in tol./xyl.)	25	Starved joint	200–320	?	Poor	3	(±31)	100	(±0)
	Lascaux MfC (in water)	25	20–40	100–160	≤20	Excellent	109	(±69)	45	(±34)
PVAl	Mowiol 3-83 (in water)	25	10–20	60–250	?	Good	22	(±12)	97	(±3)
PVAc	Mowilith 50 (in toluene)	20	Starved joint	200–320	≤50	Poor	2	(±33)	100	(±0)
	Mowilith DMC2 (in water)	10	30–180	30–50	0	Excellent	129	(±44)	68	(±12)

Any '?' identifies results that remained unclear due to a lack in visual discernibility between the consolidant and its adjacent material. '*' identifies those consolidants which softened the fracture surfaces as such that no gaps were left between the bonded surfaces

Discussion

The aim of stabilising a damaged coating layer beyond its original mechanical strength properties is generally to be approached with careful and critical consideration in the field of art conservation. This is particularly the case given the difficulties with achieving uniform consolidant penetration, which was shown to be the case with many of the consolidants tested. Therefore, tough adhesives and consolidants are not necessarily desirable for many applications. When comparing the suitability of the various consolidants, all the individual results of the reported tests need to be taken into account simultaneously, leading to the qualitative summary of the consolidant performance as shown in Table 3.

With respect to restoring the fracture properties of protein-bound foundation layers of multilayered decorative coatings which contain protein-bound foundation layers, the most promising results were achieved by the isinglass and hide glue solutions.

If it is required to re-establish the previous fracture behaviour of the material, a consolidant has to be chosen that can give similar fracture energy levels after application. This criterion is fulfilled by the isinglass and the hide glue, which also showed an average of 25 % of new failure that occurred in both unconsolidated and consolidated areas of the specimens. This behaviour suggested relatively uniform fracture properties throughout the foundation layer comprising both unconsolidated and consolidated areas. Such consolidants would thus be desirable if a fragile material was to be stabilised and some risk of new damage in surrounding, unconsolidated areas were acceptable. Addition of starch to isinglass increased the G_{Ic} of the foundations as it provided very effective bonding in the joints, however, with the disadvantage of creating an even higher risk for future damage in so far unconsolidated areas of the foundation.

Even though cold-liquid fish glue has often been used for consolidation purposes for its reputed mechanical strength [47, 48], it cannot be recommended as a consolidant for porous foundation layers when diluted to 13.3 % solid content. Not only has this study shown its inferiority in mechanical properties in comparison with other protein glues, but these findings are also supported by a comprehensive review of previously published data on protein-based glues [49].

All consolidants based on polymers dissolved in hydrocarbon solvents failed at very low loads between the re-adhered old fracture surfaces due to consolidant starvation. Such consolidants, which induce very low G_{Ic} values when applied in a single application at the given solution concentration (e.g. Paraloid, Mowilith 50), may not practically be useful as fracture will reoccur upon the

Table 3 Summary of the consolidant performance for protein-bound foundations of East Asian lacquer coatings [2]

Consolidant	Solvent	Concentration (wt%)	Effective adhesive	Effective penetrant	Toughening effect
Isinglass	water	10	+	+	0
Fish glue	water	22.5	x	+	−
Hide glue	water	10	+	+	0
Isinglass/starch	water	13.3	++	+	+
Paraloid B72	toluene	25	x	++	−−
Paraloid B72	acetone	25	x	+	−−
Paraloid B48N	toluene/xylene	25	x	++	−−
Lascaux MfC	water	25	++	+	++
Mowiol 3-83	water	25	+	+	−
Mowilith 50	toluene	20	x	++	−−
Mowilith DMC2	water	10	++	x	++

Fields marked with '+' and '++' specify whether adhesive properties and penetration ability are good or very good, respectively. In the same columns, 'x' indicates the lack of effective adhesion or penetration. The toughening effect refers to the change in fracture energy, ΔG_{Ic}, induced by consolidation and is distinguished by '0' (more or less unchanged), '+' (increased), '++' (much increased), '−' (reduced) and '−−' (starved joints which gave low G_{Ic} values under these conditions)

addition of only a small amount of energy to the system. Such energy levels are easily reached (and exceeded) during ordinary object handling and could also be induced by RH changes that give rise to stresses capable of creating further problems. Despite giving relatively low G_{Ic} values, almost half those of the original fracture energy of the foundation, the Mowiol 3-83 may still have useful properties. This formulation has the advantage of failing reliably and almost entirely within the bondline whilst providing some, albeit small, degree of stabilisation. Thus, if reliable fracture within areas of previous damage is categorically desired, a consolidant like Mowiol 3-83 may be an appropriate choice.

Similar considerations apply to the consolidants that demonstrated very effective bonding between the re-adhered fracture surfaces, inducing large increases in resistance to fracture of the stabilised foundation, i.e. Lascaux MfC, Mowilith DMC2 and (to some degree) isinglass/starch. Such high strength improvements may be desirable in specific cases, e.g. where layers are particularly load-bearing. However, if these consolidants lack penetration ability entirely (like the Mowilith DMC2) or fail to disperse uniformly within the structure, they pose the risk of creating areas with very different mechanical properties within the specimen that might induce further damage with time. This highlights that it is vital to choose consolidants on the most appropriate balance of properties, rather than a single criterion.

With regards to equilibration times, there are strong indications that the fracture energy for all tested types of polymer formulations is likely to increase further over time—at least up to a certain extent. However, the data currently available are still insufficient to draw any comprehensive conclusions of whether curing of the consolidants continues over a long period. Hence, further research on the long-term performance of the consolidants will be required.

Conclusions

The tests reported in this paper have demonstrated that a fracture mechanics approach to characterising and analysing the mechanical performance of the consolidants used to stabilise fragile protein-bound foundation layers offers great potential for the field of conservation. With the adapted DCB method, the fracture energy (an independent material property) of brittle gesso-type foundation layers was successfully measured both before and after consolidation with different polymer formulations. Measurable differences induced by the consolidants could be established, despite increased inhomogeneity within the consolidated specimens revealed during second-phase fracture. Using the same specimen for pre- and post-consolidation fracture tests was shown to be of great advantage in the testing of inhomogeneous materials such as manually applied decorative coatings on wood, facilitating direct comparison between individual specimens and significantly reducing the scatter of values measured for a complete specimen set. Comparison between failure loci on the fracture surfaces produced during both test phases, as well as between the stability and rate of crack growth, provided additional information on the mechanical properties of the material and the uniformity of the consolidation treatment.

Previously, details of the mechanical behaviour of unconsolidated and consolidated coatings could not easily and reliably be attained by conservators. This research demonstrates that the methodology used has a wide scope

for gaining a much-improved understanding of the fracture behaviour of fragile foundation layers and the strengthening ability of different consolidants. This new approach thus appears to be a promising step towards a better understanding of the fracture behaviour of fragile coatings and the strengthening potential of consolidant formulations.

References

1. Schellmann NC, Taylor AC (2011) A fracture mechanics approach for analysing failing multilayered decorative coatings on wood for evaluating suitable consolidants. In: Bridgland J (ed) ICOM-CC 16th Triennal Conference preprints, Lisbon 19–23 Sept 2011. Critério-Artes Gráficas, Lda., Lisbon

2. Schellmann NC, Taylor AC (2011) The effect of consolidants on the mechanical fracture behaviour of gesso-type foundations in multilayered decorative coatings. In: Online Proceedings of CCI Symposium 2011, Adhesives and Consolidants for Conservation: Research and Applications. Canadian Conservation Institute, Ottawa. http://www.cci-icc.gc.ca/discovercci-decouvriricc/PDFs/Paper%2019%20-%20Schellmann%20and%20Taylor%20-%20English.pdf

3. ECCO (2002) Professional guidelines. European Confederation of Conservator-Restorers' Organisations, Brussels

4. ICOM (2006) Code of ethics for museums. International Council of Museums, Paris

5. Schellmann N (2012) Consolidation of stressed and lifting decorative coatings on wood—the effect of consolidant choice on the structural integrity of multilayered East Asian lacquer coatings with gesso-type foundations. Doctoral thesis, Academy of Fine Arts Dresden

6. Simon S (2001) Die Evaluierung von Produkten und Verfahren zur Wandmalereikonservierung als konservierungswissenschaftliche Fragestellung. In: Pursche J (ed) Konservierung von Wandmalerei—Reaktive Behandlungsmethoden zur Bestandserhaltung. Karl M Lipp Verlag, München, pp 48–60

7. Rivers S, Umney N (2003) Conservation of furniture. Butterworth-Heinemann, Oxford/Auckland, chapters 8, 12

8. Rosenqvist AM (1963) New methods for the consolidation of fragile objects. In: Thomson G (ed) Recent advances in conservation. Contributions to the IIC Rome conference, 1961. Butterworths, London, pp 140–144

9. Schellmann N (2011) Delamination and flaking East Asian export lacquer coatings on wood substrates. In: Rivers S, Faulkner R, Pretzel B (eds) East Asian lacquer: material culture, science and conservation. Archetype, London, pp 107–120

10. Down J, Lafontaine R (1980) A preliminary report on the properties and stability of wood adhesives. CCI furniture and wooden objects symposium, Ottawa, 2–3 July 1980. Canadian Conservation Institute, Ottawa, pp 55–64

11. Schniewind AP, Kronkright DP (1984) Strength evaluation of deteriorated wood treated with consolidants. In: Brommelle N, Pye EM, Smith P, Thompson G (eds) Adhesives and consolidants. Preprints of the contributions to the Paris Congress, 2–8 September 1984. International Institute for Conservation, pp 146–150

12. Cuany F, Schaible V, Schießl U (1989) Studien zur Festigung biologisch geschwächten Nadelholzes: Eindringvermögen, Stabilitätserhöhung und feuchtephysikalisches Verhalten. Zeitschrift für Kunsttechnologie und Konservierung 3:249–292

13. Wang Y, Schniewind AP (1985) Consolidation of deteriorated wood with soluble resins. J Am Inst Conserv 24:77–91. doi:10.1179/019713685806028141

14. Down JL, MacDonald MA, Tétreault J, Williams RS (1996) Adhesive testing at the Canadian Conservation Institute: an evaluation of selected poly(vinyl acetate) and acrylic adhesives. Stud Conserv 41:19–44. doi:10.1179/sic.1996.41.1.19

15. Schniewind AP (1998) Consolidation of wooden panels. In: Dardes K, Rothe A (eds) The structural conservation of panel paintings. Conference proceedings, J Paul Getty Museum, April 1995. The Getty Conservation Institute, Los Angeles, pp 87–107

16. Sindlinger-Maushardt K, Petersen K (2007) Methylcellulose als Klebemittel für die Malschichtfestigung auf Leinwandbildern—Untersuchungen zur Klebkraft und zur mikrobiellen Resistenz. Zeitschrift für Kunsttechnologie und Konservierung 21:371–382

17. Berger GA (1972) Testing adhesives for the consolidation of paintings. Stud Conserv 17:173–194. doi:10.1179/sic.1972.016

18. Katz KB (1985) The quantitative testing and comparisons of peel and lap/shear for Lascaux 360 H.V. and Beva 371. J Am Inst Conserv 24:60–68. doi:10.1179/019713685806028097

19. Bradley S (1984) Strength testing of adhesives and consolidants for conservation purposes. In: Brommelle N, Pye EM, Smith P, Thompson G (eds) Adhesives and consolidants. Preprints of the contributions to the Paris Congress, 2–8 September 1984. International Institute for Conservation, London, pp 22–25

20. Shashoua YR (1993) Mechanical testing of resins for use in conservation. Preprints of the ICOM-CC 10th Triennial Meeting, Washington, 22–27 August 1993. ICOM Committee for Conservation, pp 580–585

21. Berger GA, Zeliger HI (1984) The procedure of developing an adhesive for paintings: the importance of valid tests. In: Brommelle N, Pye EM, Smith P, Thompson G (eds) Adhesives and consolidants. Preprints of the contributions to the Paris Congress, 2–8 September 1984. International Institute for Conservation, London, pp 13–17

22. Down JL (1996) Epoxy resin adhesives: report on shear strength retention on glass substrates. J Int Inst Conserv Can Group 21:28–35

23. Wong L, Bicer-Simsir B, Yuan H, Qing C (2011) Testing the performance of a traditional Chinese adhesive for the conservation of Qing dynasty painted architectural decoration at Shuxiang Temple, Chengde. In: Bridgland J (ed) ICOM-CC 16th Triennial Conference preprints, Lisbon 19–23 Sept 2011. Critério-Artes Gráficas, Lda., Lisbon

24. Kinloch AJ (1987) Adhesion and adhesives: science and technology. Chapman and Hall, London

25. Hashemi S, Kinloch AJ, Williams JG (1990) Mechanics and mechanisms of delamination in a poly(ether sulphone)-fibre composite. Compos Sci Technol 37:429–462. doi:10.1016/0266-3538(90)90013-U

26. River BH, Okkonen EA (1993) Contoured wood double cantilever beam specimen for adhesive joint fracture tests. J Test Eval 21:21–28. doi:10.1520/JTE11737J

27. River BH (1994) Fracture of adhesive-bonded wood joints. In: Pizzi A, Mittal KL (eds) Handbook of adhesive technology. Marcel Dekker Inc, New York, pp 151–177

28. Blackman BRK, Dear JP, Kinloch AJ et al (1995) The failure of fibre composites and adhesively bonded fibre composites under high rates of test. Part I: mode I loading—experimental studies. J Mater Sci 30:5885–5900. doi:10.1007/BF01151502

29. Bader MG, Hamerton I, Hay JN, Kemp M, Winchester S (2000) Double cantilever beam testing of repaired carbon fibre composites. Compos Part A Appl Sci Manuf 31:603–608. doi:10.1016/S1359-835X(99)00095-0

30. Gagliano JM, Frazier CE (2001) Improvements in the fracture cleavage testing of adhesively-bonded wood. Wood Fiber Sci 33:377–385

31. Brunner AJ, Blackman BRK, Davies P (2008) A status report on delamination resistance testing of polymer-matrix composites. Eng Fract Mech 75:2779–2794. doi:10.1016/j.engfracmech.2007.03.012

32. BS7991 (2001) Determination of the mode I adhesive fracture energy G_{Ic} of structural adhesives using the double cantilever beam (DCB) and tapered double cantilever beam (TDCB) specimens. BSI, London

33. Blackman BRK, Kinloch AJ, Paraschi M, Teo WS (2003) Measuring the mode I adhesive fracture energy, G_{Ic}, of structural adhesive joints: the results of an international round-robin. Int J Adhes Adhes 23:293–305. doi:10.1016/S0143-7496(03)00047-2

34. Knaebe M, Williams RS (1993) Determining paint adhesion to wood using a uniform double-cantilever beam technique. J Test Eval 21:272–279. doi:10.1520/JTE11952J

35. Schramm H-P, Hering B (1988) Historische Malmaterialien und ihre Identifizierung. Akademische Druck- und Verlagsanstalt, Graz

36. Lehmann M (2004) Langfristige Schädigung von Wandmalerei durch die Wirkung eingebrachter Kunststoffe am Beispiel der Gewölbemalereien in der Krypta der Quedlinburger Stiftskirche St. Servatius. Zeitschrift für Kunsttechnologie und Konservierung 18:71–92

37. Blackman BRK, Kinloch AJ (2001) Fracture tests for structural adhesive joints. In: Pavan A, Moore DR, Williams JG (eds) Fracture mechanics testing methods for polymers, adhesives and composites. Elsevier Science, Amsterdam

38. Blackman BRK, Kinloch AJ (2001) Linear-elastic fracture-mechanics (LEFM) test protocols download: DCB (LB) spreadsheet (Excel). http://www3.imperial.ac.uk/meadhesion/testprotocols/lefm. Accessed 10 February 2014

39. Reiterer A, Tschegg S (2002) The influence of moisture content on the mode I fracture behaviour of sprucewood. J Mater Sci 37:4487–4491. doi:10.1023/A:1020610231862

40. Friedrich K, Karsch UA (1981) Failure processes in particulate filled polypropylene. J Mater Sci 16:2167–2175. doi:10.1007/BF00542377

41. Lencz B (2005) The development of conservation of Japanese armors and lacquerware in Hungarian public collections. The role of Urushi in international exchange. In: Proceedings of the 27th international symposium on the conservation and restoration of cutural property, 3–5 December 2003. National Research Institute for Cultural Properties/Tokyo National Museum, pp 191–200

42. Breidenstein I (2000) Konzeptionelle Überlegungen zur Restaurierung eines Chinesischen Lackparavents. In: Kühlenthal M (ed) Japanische und Europäische Lackarbeiten/Japanese and European lacquerware. Lipp, München, pp 561–585

43. Springob C (2001) Stärkekleister als Verdickungsmittel von Störleim zur Malschichtfestigung. Zeitschrift für Kunsttechnologie und Konservierung 15:111–132

44. Sakuno T, Schniewind AP (1990) Adhesive qualities for consolidants for deteriorated wood. J Am Inst Conserv 29:33–44. doi:10.1179/019713690806046127

45. Hedlund HP, Johansson M (2005) Prototypes of Lascaux's medium for consolidation: development of a new custom-made polymer dispersion for use in conservation. Restauro 111:432–439

46. POLYKON (2014) Mowilith DMC2. Fachhochschule Potsdam, Studiengang Konservierung und Restaurierung. http://polykon.fh-potsdam.de/polymer.php?id=235&page=eigenschaften. Accessed 25 March 2014

47. Webb M (2000) Lacquer—technology and conservation. Butterworth-Heinemann, Oxford

48. Breu Z, Miklin-Kniefacz S (1995) Bericht zur Restaurierung des Lackparavents aus dem Napoleonzimmer Schloss Schönbrunn, Wien. In: Miklin-Kniefacz S (ed) Zur Restaurierung der Vieux-lacque-Tafeln in Schönbrunn: Grundlagen und Vorarbeiten. Schloss Schönbrunn, Wien, pp 7–13

49. Schellmann N (2007) Animal glues: a review of their key properties relevant for conservation. Rev Conserv 8:55–66. doi:10.1179/sic.2007.52.Supplement-1.55

50. Miklin-Kniefacz S (1995) Untersuchungsbericht über geeignete Klebemedien zur Schollenniederlegung an ostasiatischen Lacktafeln. In: Miklin-Kniefacz S (ed) Zur Restaurierung der Vieux-lacque-Tafeln in Schönbrunn: Grundlagen und Vorarbeiten. Schloss Schönbrunn, Wien, pp 16–21

51. Webb M (1998) Methods and materials for filling losses on lacquer objects. J Am Inst Conserv 37:117–133. doi:10.1179/019713698806082930

52. Breidenstein I (2002) 'Sawed, divided, cut, cleft and split asunder': eighteenth-century Chinese export lacquer screens in Europe—two restoration cases. In: van Duin P, Piena H (eds) The meeting of the East and West in the furniture trade, 6th international symposium on wood and furniture conservation (conference proceedings). Stichting Ebenist, Amsterdam, pp 59–64

53. Kato H (1988) The restoration of urushiware for export with animal glue and urushi. In: Brommelle NS, Smith P (eds) Urushi—proceedings of the Urushi Study Group, 10–27 June 1985, Tokyo, Japan. The Getty Conservation Institute, Marina del Rey, pp 81–84

54. Yamasaki K (1957) Review of conservation of old art objects in Japan. Stud Conserv 3:83–88

55. Chase WT (1988) Lacquer examination and the treatment at the Freer Gallery of Art: some case histories. In: Brommelle NS, Smith P (eds) Urushi—proceedings of the Urushi Study Group, 10–27 June 1985, Tokyo, Japan. The Getty Conservation Institute, Marina del Rey, pp 95–111

56. Chase WT, Jett PR, Koob SP, Norman J (1988) The treatment of a Chinese red lacquer stationery box. In: Mills JS, Smith P, Yamasaki K (eds) The conservation of Far Eastern art. Preprints of the contributions to the Kyoto Congress, 19–23 September 1988. International Institute for Conservation, London, pp 142–145

57. Gillis KZ (1998) After the deluge: the conservation of two Chinese chests. WAG Postprints—Alexandria, Virginia. Amerian Institute for Conservation Wooden Artifacts Group, Washington

58. Hagedorn B (2002) Zur Restaurierung eines französischen Lackmöbels aus Schloss Wilhelmsthal/Restoring a French lacquered bureau from Wilhelmsthal Palace. In: Kühlenthal M (ed) Japanische und Europäische Lackarbeiten/Japanese and European lacquerware. Lipp, München, pp 517–536